Molecular Biotechnology
https://doi.org/10.1007/s12033-024-01107-8

ORIGINAL PAPER

The Up-Regulated Expression of Mitochondrial Membrane Molecule RHOT1 in Gastric Cancer Predicts the Prognosis of Patients and Promotes the Malignant Biological Behavior of Cells

Fanhao Kong[1] · Siwen Yang[1] · Ruimeng Shi[1] · Yanyu Peng[2]

Received: 9 December 2023 / Accepted: 30 January 2024

Abstract

Gastric cancer (GC) remains a major disease of high morbidity and mortality worldwide despite advances in diagnosis and treatment. Ras homolog family member T1 (RHOT1) plays an important role in several cancers. Our study aimed to analyze RHOT1 expression, to assess the relationship between its expression and the prognosis of patients, and know the impact of RHOT1 on GC cells. The Cancer Genome Atlas (TCGA) RNA-seq data was used for gene expression analysis, survival and prognostic analysis. Nomograms were created to analyze the pathological factors of GC patients. RHOT1 expression was up-regulated by analyzed TCGA-Stomach adenocarcinoma (STAD) data and verified by Polymerase Chain Reaction (PCR) assay in GC tissues and cell lines. Furthermore, RHOT1 up-regulation was significantly associated with shorter survival of GC patients. At last, after silencing the expression of RHOT1 in AGS cell lines, we found that the proliferative ability of the cells was significantly reduced, the cell invasion ability was significantly inhibited, the cell migration ability was also significantly weakened, the cell cycle was arrested in the G0/G1 phase, and apoptosis was significantly increased. So RHOT1 could impact the apoptosis, proliferation, invasion, and migration behavior of GC cells. We trust RHOT1 has the potential to become a new oncogene biomarker for diagnosis and prognosis as well as a new therapeutic target in GC.

Keywords RHOT1 · Gastric cancer · Biomarker · Prognosis · Migration · Invasion

Abbreviations

ACC	Adrenocortical carcinoma
BLCA	Bladder urothelial carcinoma
BRCA	Breast invasive carcinoma
CESC	Cervical squamous cell carcinoma and endocervical adenocarcinoma
CHOL	Cholangiocarcinoma
COAD	Colon adenocarcinoma
DLBC	Lymphoid neoplasm diffuse large B-cell lymphoma
ESCA	Esophageal carcinoma
GBM	Glioblastoma multiforme
HNSC	Head and neck squamous carcinoma
KICH	Kidney chromophobe
KIRC	Kidney renal clear cell carcinoma
KIRP	Kidney renal papillary cell carcinoma
LAML	Acute myeloid leukemia
LGG	Lower grade glioma
LIHC	Liver cancer
LUAD	Lung adenocarcinoma
LUSC	Lung squamous cell carcinoma
MESO	Mesothelioma
OV	Ovarian cancer
PAAD	Pancreatic cancer
PCPG	Pheochromocytoma & paraganglioma
PRAD	Prostate cancer
READ	Rectal cancer
SARC	Sarcoma
SKCM	Melanoma
STAD	Stomach cancer
TGCT	Testicular cancer
THCA	Thyroid cancer
THYM	Thymoma
UCEC	Endometrioid cancer

✉ Yanyu Peng
yypeng@cmu.edu.cn

[1] Shenyang Medical College, Shenyang, Liaoning, People's Republic of China

[2] Department of Histology and Embryology, Shenyang Medical College, Shenyang, Liaoning, People's Republic of China

Published online: 06 March 2024

UCS Uterine carcinosarcoma
UVM Ocular melanomas

Introduction

Gastric cancer (GC) is widely recognized as a highly lethal malignancy, characterized by significantly elevated morbidity and mortality rates. According to the comprehensive analysis of 185 nations and 36 types in the Global Cancer Statistics report, GC continues to maintain its position as the fifth most prevalent cancer globally and ranks fourth in terms of GC-related deaths [1]. Despite advancements in early-stage diagnosis and treatment for GC, the five-year overall survival rate remains disappointingly low due to its aggressive malignant behavior [2]. At present, the upper gastrointestinal endoscopy strategy has been perfected as the gold standard for the diagnosis of GC [3]. However, upper gastrointestinal (GI) endoscopy is an invasive strategy that requires precise instruments and proficient manipulators enabling it not to be common in some areas. So the majority of GC patients are often diagnosed during intermediate or advanced stages, leading to missed opportunities for timely intervention [4]. Surgery remains the primary therapeutic approach for managing GC [5]. Succinctly stated, there is an urgent need to identify biomarkers for early detection and explore the molecular mechanisms underlying the progression of GC.

RHOT1 plays a crucial role in maintaining the balance of mitochondria and apoptosis as an important member of atypical Rho GTPase s[6]. Mitochondrial clustering occurs after RHOT1 mutation since RHOT1 links mitochondria to the transportation mechanism of microtubules [7]. A study demonstrated that RHOT1 regulates mitochondrial transport in hippocampal neurons through the recruitment of receptor interacting factor-1 (Grif-1) by GTPase activity [8]. Furthermore, PTEN induced putative kinase 1 (PINK1) is capable of hindering mitochondrial movement by phosphorylating and degrading RHOT1 [9]. These findings suggest that RHOT1 could have a crucial function in the mitochondrial membrane of cells. Increasing evidence confirmed that RHOT1 was involved in cancer progression. A study reported that RHOT1 was correlated with lymph node metastasis, overall survival, migration, and proliferation in pancreatic cancer [10, 11]. Researchers found that interfering with the myelocytomatosis oncogene Myc/RHOT1 pathway blocked the recruitment of mitochondria in the cortical cytoskeleton of tumor cells, reducing the invasion and metastasis of cancer cells [12]. Our prior research verified the existence of particular binding sites between miRNA-1299 and RHOT1 via dual luciferase assay [13]. We observed that the influence of hsa_circ_0005230 upon GC cell proliferation, apoptosis, invasion, and migration behavior was significantly affected by the miR-1299/RHOT1 axis. Our next step will be to confirm the functional oncogene RHOT1 in GC malignant behavior.

Previous research found that RHOT1 expression was upregulated in the mRNA and protein levels in GC tissue. In this study, we utilized bioinformatics methods to conduct Pan-cancer analysis and RHOT1 expression in large-scale sample tissues, screening for independent risk factors to explore the prognosis and survival of GC patients. We also examined RHOT1 expression in the (MGC-803, SNU-1 and AGS cell lines). After silencing the gene, we performed Cell Counting Kit-8 (CCK-8), wound healing, flow cytometry, Transwell invasion and migration cytological assays to assess cell capacity changes. Lastly, we discussed the potential mechanism of RHOT1 in GC cells.

Methods

Data Acquisition and Processing for Gene Expression Analysis

Data for 33 types of cancer (Pan-cancer) were acquired from The Cancer Genome Atlas (TCGA) website (https://portal.gdc.cancer.gov/). Subsequently, TCGA-STAD contained 375 cases of GC and 32 adjacent non-cancerous tissues RNA sequencing data was in HTSeq-FPKM (Fragments Per Kilobase per Million) format at level 3 and was transformed to TPM (Transcripts Per Million reads) format before being converted to log2 [14]. A total of more than 60,000 RNA was detected, and only protein coding RNA was screened. The analysis of data comprised 174 normal tissues from Genotype-Tissue Expression (GTEx), 36 adjacent non-cancerous tissues, and 414 GC tissues. The data were acquired from UCSC XENA (https://xenabrowser.net/datapages/), and any unavailable or unknown clinical information was considered as default value filled by "NA". RNA-seq data from TCGA pan-cancer (including STAD) and GTEx normal tissues were utilized to investigate the differential expression of RHOT1 among various sample tissues via boxplot. Visualization was conducted using R software [version 4.3.0] in conjunction with the R packages "Deseq2" and "ggplot2" [version 3.3.3].

Correlation Analysis Between Clinicopathological Factors and Gene Expression

The RHOT1 mRNA expression levels of STAD patients were analyzed using R software [version 3.6.3] based on the TCGA database and clinical information such as gender, age, histological grade, World Health Organization (WHO) histological types, pathological stage, lymph node

metastasis, depth of infiltration grade, anatomical neoplasm subdivision, and distant metastasis of the GC patients.

Survival and Prognostic Analysis

Survival analyses were presented using the Kaplan–Meier (KM) curves method, with log-rank tested using the "survival" package (https://CRAN.R-project.org/package=survival) [15] and results visualized using the "survminer" package. The groups were divided into low and high-expression groups using the median RHOT1 expression. Clinical data for GC was analyzed using univariate Cox analysis with R software, and risk ratios (HR) and *P* values of clinical factors were calculated. Clinical factors with $P < 0.1$ were considered for multivariate Cox analysis. The prognostic nomogram [16] with histologic grade, age, and pathologic stage features) were plotted using the rms package [version 6.2-0] and the survival package [version 3.2-10]; the prognostic type was overall survival (OS). The calibration visualization parameters were set to the number of samples per group for repeated calculations (40); number of repeated calculations (200); and method (boot).

Cell Lines and Cell Culture

Cell lines were AGS, MGC-803, SNU-1, and GES-1 (Servicebio, Immocell, China) (batch of cells: IM-H084202303). AGS cell line was cultured using DMEM/F12 medium (Gibco, USA), MGC-803 cell line was cultured using DMEM/H medium (Gibco, USA), and GES-1 cell line was cultured using RPMI 1640 medium (Gibco, USA), adding 10% fetal bovine serum (FBS, Clark bioscience), 100 U/mL penicillin, and 100 µg/mL streptomycin at 37 °C in 5% CO_2.

Total RNA Extraction and Quantitative Real-Time PCR (qRT-PCR)

The cells were washed with PBS and collected for RNA isolation. Following the reference protocol, under RNase-free conditions, the RNA Easy Fast Tissue/Cell Kit (Tiangen, China) was prepared for total RNA extraction. The quality of RNA was assessed by evaluating the optical density (OD) of 260 nm/280 nm. A total of 1000 ng qualified mRNA was reversed transcribed by PrimeScirpt RT Master Mix Kit (Takara, China) into cDNA, and SYBR Green Master Mix Kit (Takara, China) was adopted to detect the relative expression of mRNA, calculated using the $2^{-\Delta\Delta C_t}$ method. All primer sequences were documented in the Supplementary Table. RHOT1 expression was standardized by GAPDH. Each sample was performed in triplicate in 7500Fast (ABI, USA).

siRNA Transfection

The target-specific siRNA(si-RHOT1) sequence was presented in the Supplementary Table and negative control (NC) was purchased from GenePharma (China) and transfected into AGS cell line cultured in six-well plates. One day before transfection, AGS cell was seeded to reach approximately 70% confluence in the medium (Gibco, USA). The siRNA was transfected into the AGS cells with 20 nM by Lipo 6000 (Beyotime, China) transfection reagent diluted by Optimem. After 48 h, the silencing efficiency of RHOT1 mRNA expression was evaluated by qRT-PCR.

CCK-8 Proliferation Assay

Cell Counting Kit-8 (CCK-8) (MCE, USA) was used to detect the proliferation of AGS cells. We seeded approximately 2×10^3 cells in 100 µL on a 96-well plate and incubated at 37 °C. The CCK-8 reagent (10 µL) was mixed into each well at 0, 24, 48, 72, and 96 h, and incubation was carried out at 37 °C for 2.5 h. OD values at 450 nM were read by a microplate reader (Molecular Devices, USA).

Flow Cytometry

To assess the cell cycle and apoptosis of the cells, a flow cytometry assay was performed [17]. The AGS cells, about 1×10^6 each tube, were stained with propidium iodide (PI) (Beyotime, China) for the cell cycle test and the test of apoptosis utilized Annexin-V and PI (Beyotime, China). The cells were stained at 37 °C for 30 min in the dark using PI for the cell cycle and Annexin-V and PI for apoptosis. The percentage of apoptotic cells was measured as the sum of Q2 and Q3 and the cell cycle was analyzed using the Dean–Jett–Fox model [18]. FACSCalibur and FACSCelesta (BD, USA) were used to detect cell cycle and apoptosis, respectively. The data were analyzed using FlowJo v10.6.2.

Wound Healing Assay

The migration abilities of AGS cells were assessed using a wound healing assay. 3×10^5 cells/mL were cultured per well in the 12-well plate. After 6 h of incubation to reach more than 90% confluence, 1 mL of cell suspension was added to the 12-well plate, 200 µL pipette tip was used to scrape the cell-free area, PBS was washed 2–3 times, 2% serum medium was prepared, and the scratch wounds were recorded under the microscope at 0, 24, and 48 h.

Transwell Assay

In the Transwell invasion assay, matrigel gel (BD, USA) was diluted with a serum-free medium at a ratio of 1:7. The final

50 µL of dilution was put into a Transwell (Corning, USA) and incubated at 37 °C for 1 h. In the Transwell migration assay, 200 µL of cell suspension was transferred into a transwell (Corning, USA) upper chamber without matrigel gel, and 500 µL of medium with 20% FBS was transferred into a transwell lower chamber and incubated with 5% CO_2 in a 37 °C incubator for 48 h. After incubation, a 4% paraformaldehyde solution was used to fix the cells in the transwell. The transwell was subsequently stained with 0.1% crystal violet for 20 min. Cell counts were recorded for migration and invasion through bright field microscopy using ImageJ.

Statistical Analysis

Parametric comparisons were conducted using Student t-tests, while nonparametric tests for two independent samples were performed using the Mann–Whitney *U* test. Additionally, the Wilcoxon test was utilized to compare non-normal data. The χ^2 test was employed to compare groups, and Fisher's exact probability method was used when the χ^2 test was not appropriate. Survival curves were plotted using the Kaplan–Meier method, survival rates were compared between groups with the log-rank test, and independent risk factors were evaluated with univariate and multivariate Cox regression analysis. The significance level was determined to be $P < 0.05$.

Results

RHOT1 Expression in Pan-Cancer and GC

The transcriptome data from TCGA and GTEx samples were analyzed to determine RHOT1 expression. Initially, 33 TCGA tumors were analyzed at the Pan-cancer level. As shown in Fig. 1a, RHOT1 exhibited significant differential expression in BRCA, CHOL, COAD, ESCA, HNSC, KICH, LIHC, LUAD, LUSC, PRAD, STAD, THCA, and UCEC compared to the adjacent non-cancer tissues (Normal group). Among these, RHOT1 showed down expression in BRCA, KICH, LUAD, LUSC, PRAD, THCA, and UCEC, and high expression in CHOL, COAD, ESCA, HNSC, LIHC, and STAD. A total of 407 TCGA samples were chosen for unpaired expression analysis, As illustrated in Fig. 1b, RHOT1 expression was markedly elevated in GC in comparison to the adjacent non-cancerous (normal group). The difference in median values between the two groups was 0.352 (0.099–0.62) and the difference was statistically significant ($P = 0.005$). After analyzing the combined transcriptomic data of TCGA and GTEx, consisting of 624 samples, unpaired expression differences in GC were evaluated and compared with the normal group including adjacent non-cancer and normal. RHOT1 expression was found to be significantly up-regulated in GC, with a median difference of 0.246 (0.155–0.338) between the two groups. This difference was statistically significant ($P < 0.001$) as presented in Fig. 1c. The expression of RHOT1 mRNA in GC was confirmed using PCR. The results, as demonstrated in Fig. 1d, indicated up-regulation of RHOT1 mRNA expression in AGS, MGC-803, and SNU-1 cell lines when compared to GES-1.

Analysis of Clinicopathological Factors

The study utilized data from 375 cases downloaded from TCGA. Cases were divided into low and high-expression groups using the median value of RHOT1 expression. Table 1 presented the correlation between RHOT1 expression levels and clinicopathological factors. The analysis revealed significant correlations between high RHOT1 expression and race ($\chi^2 = 8.02$, $P = 0.018$) as well as WHO's histological types ($\chi^2 = 11.1$, $P = 0.049$). Specifically, RHOT1 expression was found to oppose the trend of Asian or White populations among racial factors, but not among Blacks or African-Americans. Pathological factors such as gender, age, histologic grade, depth of infiltration, distant metastasis, and site of onset did not show any significance. Further analyses were conducted for certain subgroups of pathological factors. First, we analyzed the level of RHOT1 expression and lymph node metastasis. According to the Kruskal–Wallis Test, there was a statistically significant difference between groups ($P = 0.024$). The Dunn's test, which was used to correct for the significance level by the Bonferroni method, indicated that the N0 group was higher than the Normal group, as shown in Fig. 2a (*P*-value not specified). Adjacency = 0.025; The N1&N2&N3 group exhibited greater values than the Normal group ($P.adj = 0.028$) with a statistically significant difference, while the difference between the N1&N2&N3 and N0 group was not statistically significant ($P.adj > 0.05$). We examined RHOT1 expression levels in the subgroups based on the T stage using the same methodology. Our findings revealed that the T3 & T4 group showed higher levels of RHOT1 expression compared to the Normal group ($P.adj = 0.017$). Conversely, we observed no statistically significant differences in the RHOT1 expression levels between the T1 & T2 group and the Normal group, and the T1 & T2 group and the T3 & T4 group ($P.adj > 0.05$) (Fig. 2b). RHOT1 expression was analyzed within histologic grade subgroups. The G1&G2 group had significantly higher expression than the Normal group ($P.adj = 0.017$), as did the G3 group ($P.adj = 0.03$). However, there was no statistically significant difference between the expression of the G1&G2 group and the G3 group ($P.adj > 0.05$), as illustrated in Fig. 2c. Finally, in the subgroup analysis examining RHOT1 expression levels during the pathologic stage as demonstrated in Fig. 2d, the Stage I and Stage II groups

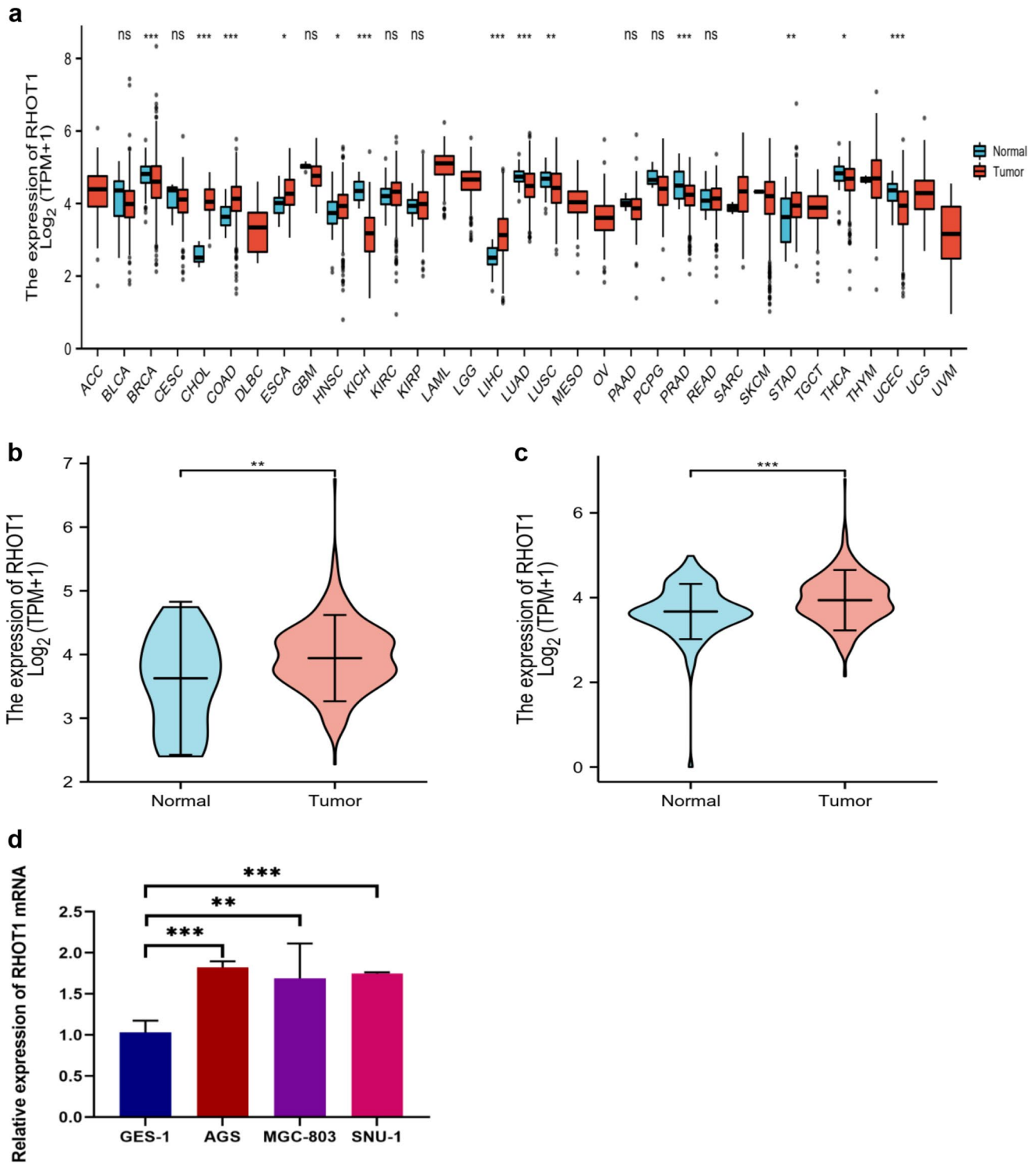

Fig. 1 Expression of RHOT1 in Pan-cancer and GC. **a** RHOT1 expression was analyzed in tumor and adjacent non-cancerous tissues in TCGA Pan-cancer. **b** Unpaired analysis of RHOT1 expression was performed in tumor and adjacent non-cancerous tissues in GC from TCGA. **c** The unpaired analysis of RHOT1 expression in tumor and Normal tissues in GC from TCGA and GTEx. **d** The expression of RHOT1 was up-regulated in GC cell lines, compared to GES-1. $^{*}P<0.05$, $^{**}P<0.01$, $^{***}P<0.001$, $n=3$

Table 1 Characteristics of patients with gastric cancer and expression RHOT1

Characteristic	Low expression of RHOT1	High expression of RHOT1	*P*
n	187	188	
Age, *n* (%)			0.371
≤ 65	87 (53%)	77 (47%)	
> 65	99 (47.8%)	108 (52.2%)	
Race, *n* (%)			0.018*
Asian	47 (63.5%)	27 (36.5%)	
Black or African American	3 (27.3%)	8 (72.7%)	
White	114 (47.9%)	124 (52.1%)	
Gender, *n* (%)			0.313
Female	72 (53.7%)	62 (46.3%)	
Male	115 (47.7%)	126 (52.3%)	
WHO'Histological type, *n* (%)			0.049*
Diffuse type	37 (58.7%)	26 (41.3%)	
Mucinous type	12 (63.2%)	7 (36.8%)	
Not otherwise specified	90 (43.5%)	117 (56.5%)	
Papillary type	1 (20%)	4 (80%)	
Signet ring type	6 (54.5%)	5 (45.5%)	
Tubular type	41 (59.4%)	28 (40.6%)	
Histologic grade, *n* (%)			0.577
G1	5 (50%)	5 (50%)	
G2	64 (46.7%)	73 (53.3%)	
G3	115 (52.5%)	104 (47.5%)	
T stage, *n* (%)			0.078
T1	12 (63.2%)	7 (36.8%)	
T2	38 (47.5%)	42 (52.5%)	
T3	95 (56.5%)	73 (43.5%)	
T4	42 (42%)	58 (58%)	
N stage, *n* (%)			0.849
N0	56 (50.5%)	55 (49.5%)	
N1	46 (47.4%)	51 (52.6%)	
N2	39 (52%)	36 (48%)	
N3	40 (54.1%)	34 (45.9%)	
M stage, *n* (%)			0.382
M0	169 (51.2%)	161 (48.8%)	
M1	10 (40%)	15 (60%)	
Pathologic stage, *n* (%)			0.156
Stage I	23 (43.4%)	30 (56.6%)	
Stage II	64 (57.7%)	47 (42.3%)	
Stage III	77 (51.3%)	73 (48.7%)	
Stage IV	15 (39.5%)	23 (60.5%)	
Anatomic neoplasm subdivision, *n* (%)			0.609
Antrum/distal	75 (54.3%)	63 (45.7%)	
Cardia/proximal	25 (52.1%)	23 (47.9%)	
Fundus/body	64 (49.2%)	66 (50.8%)	
Gastroesophageal junction	18 (43.9%)	23 (56.1%)	
Other	1 (25%)	3 (75%)	

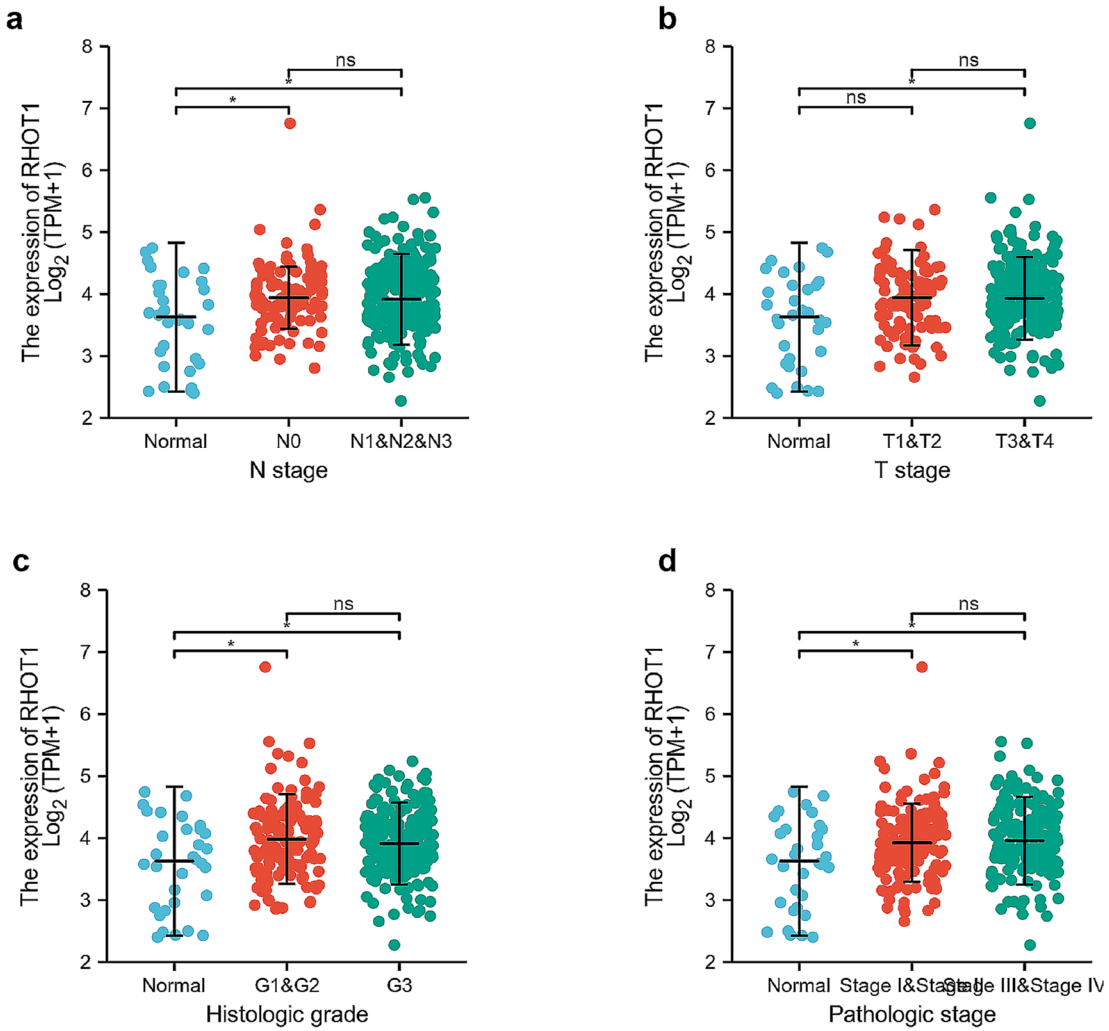

Fig. 2 The expression of RHOT1 in GC and its relationship with pathological factors. **a** The expression of RHOT1 in different subgroups of lymph node metastasis numbers. **b** T stage, **c** Histologic grade, **d** Pathologic stage. $^{*}P<0.05$, $^{**}P<0.01$, $^{***}P<0.001$

exhibited higher levels compared to the normal group (*P*. adj = 0. 049). Additionally, the Stage III and Stage IV groups had higher levels than the normal group (*P*.adj = 0.015). Moreover, statistical analysis did not indicate any significant difference between the Stage III and Stage IV groups when compared to the Stage I and Stage II groups (*P*.adj > 0.05). The results suggest that high RHOT1 expression in GC patients increases the likelihood of progression to advanced stages, indicating its potential as a favorable biomarker for clinical diagnosis and treatment of GC.

Prognostic Risk Factors of GC Cox Regression and Prognosis Analysis

Univariate and Multivariate Cox Analysis

We conducted univariate and multivariate Cox regression analyses to determine the independent prognostic factors for GC. Table 2 demonstrated that various factors, including age, histological grade, pathological stage, depth of infiltration (T), lymph node metastasis (N), distant metastasis (M), and RHOT1 expression, were identified as risk factors in the univariate Cox analysis for the OS of GC patients. These factors with P values greater than 0.1 were included as parameters in the multifactorial Cox regression analysis. The study found that age, WHO's pathological type, histological grade, and RHOT1 expression were independent prognostic factors for the OS of patients with GC. Then a Nomogram to predict the OS of the patient's survival at 1, 3, and 5 years based on these prognostic factors, as determined by multivariate Cox regression analysis (Fig. 3a). The predictive performance of the Nomogram was evaluated using calibration curves. Based on the graph in Fig. 3b, the predictions for 1 and 3 years were more favorable than for 5 years when compared to the ideal line. This indicates that a

Table 2 Univariate and multivariate COX regression analysis

Characteristics	Total(N)	Univariate analysis		Multivariate analysis	
		Hazard ratio (95% CI)*	*P* value	Hazard ratio (95% CI)	*P* value
Age	367				
≤65	163				
> 65	204	1.620 (1.154–2.276)	0.005*	2.016 (1.377–2.952)	< 0.001*
Gender	370				
Male	237				
Female	133	0.789 (0.554–1.123)	0.188		
Pathologic stage	347				
Stage I&Stage II	160				
Stage III	149	1.746 (1.193–2.554)	0.004*	1.220 (0.683–2.179)	0.502
Stage IV	38	2.933 (1.768–4.865)	< 0.001*	2.918 (1.303–6.532)	0.009*
WHO's histological types	369				
Papillary Type&Tubular Type	74				
Diffuse Type&Mucinous Type&Signet Ring Type	93	0.936 (0.572–1.530)	0.791		
Not Otherwise Specified	202	1.183 (0.772–1.812)	0.441		
Histologic grade	361				
G1&G2	144				
G3	217	1.353 (0.957–1.914)	0.087	1.526 (1.033–2.256)	0.034*
T stage	362				
T1&T2	96				
T3&T4	266	1.719 (1.131–2.612)	0.011*	1.165 (0.685–1.981)	0.573
N stage	352				
N0	107				
N1&N2&N3	245	1.925 (1.264–2.931)	0.002*	1.339 (0.736–2.435)	0.340
M stage	352				
M0	327				
M1	25	2.254 (1.295–3.924)	0.004*	0.863 (0.362–2.059)	0.740
RHOT1 expression	370				
Low	186				
High	184	1.376 (0.990–1.913)	0.058	1.550 (1.080–2.223)	0.017*

*CI denotes confidence interval

nomogram with multiple independent prognostic factors is a superior method for predicting the short-term or long-term survival of GC patients when compared to relying on a single prognostic factor.

Analysis of Survival Prognosis

After determining the best cutoff value (auto data derived from the KM plot), we classified the RHOT1 expression into two groups: high expression and low expression. Figure 3c illustrated that GC patients with high RHOT1 expression had shorter survival rates than those with low expression. Thus, their prognosis was significantly worse.

Silencing RHOT1 Inhibits Proliferation and Promotes Apoptosis in GC Cells

To investigate the functional role of RHOT1 in GC, we used specific siRNA to effectively silence its expression in AGS cells, which displayed the highest fold expression among the cell lines tested. The silencing efficiency of si-RHOT1 in AGS cells was evaluated through qRT-PCR following transfection. In Fig. 4a, it was evident that si-RHOT1 exhibited a silencing efficiency exceeding 90% when compared to the NC group. Subsequently, the proliferation of AGS was observed through a CCK-8 assay after silencing the expression of RHOT1. The outcome suggested that the proliferation of the si-RHOT1 group decreased significantly in AGS

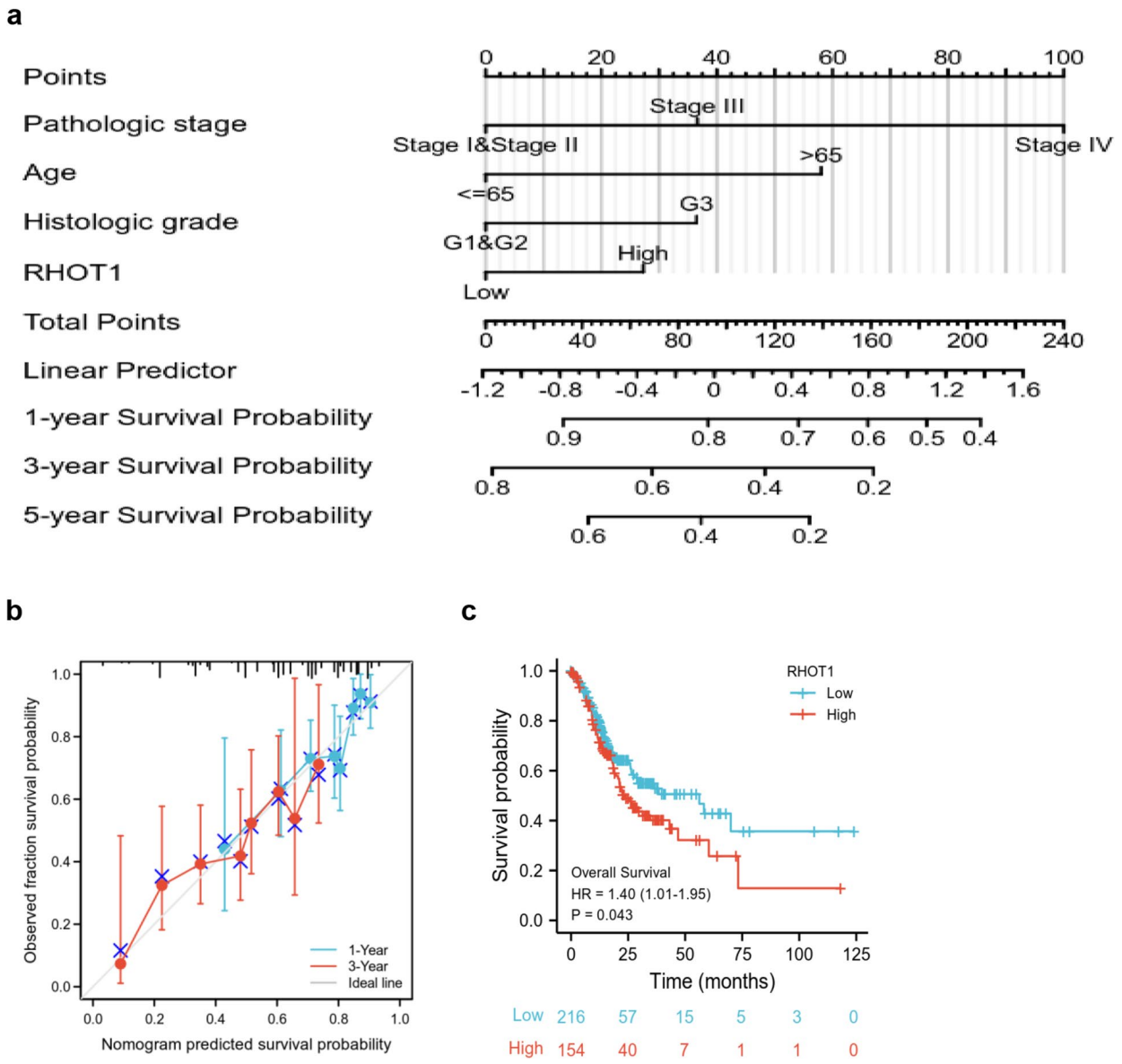

Fig. 3 Prognosis and survival analysis. **a** Multivariate Cox regression analysis of independent prognostic risk factors to perform a nomogram with GC based on TCGA. **b** Calibration curves were used to evaluate the predictive ability of prognostic risk factors consistent with the ideal line. **c** Kaplan–Meier curve indicated the relationship between RHOT1 expression and the prognosis of GC patients

after transfection at 24 h, 48 h, 72 h and 96 h ($P < 0.05$), particularly at 24 h and 48 h with a significant difference between the NC group ($P < 0.001$) (Fig. 4b). This result demonstrated that silencing RHOT1 in AGS cells reduced their ability to proliferate remarkably. The cell cycle was estimated using flow cytometry to assess changes following RHOT1 silencing in AGS cells. Figure 4c showed an increase in the proportion of cells in the G0/G1 phase and a decrease in cells in the S phase, compared to the NC group. These results suggested that silencing RHOT1 significantly arrested the G0/G1 phase while reducing DNA synthesis in the S phase, which was disadvantageous to AGS cell proliferation. Additionally, flow cytometry detected cell apoptosis to evaluate the extent of apoptosis in GC cells. Silencing RHOT1 facilitated the apoptosis of AGS cells, promoting apoptosis of AGS cells (Fig. 4d). Therefore, we could speculate silencing RHOT1 suppressed GC cell proliferation and promoted apoptosis.

Silencing of RHOT1 Inhibits the Migration and Invasion of Gastric Cells

We investigated the impact of RHOT1 on the migration and invasion of the GC cell lines. Firstly, we used

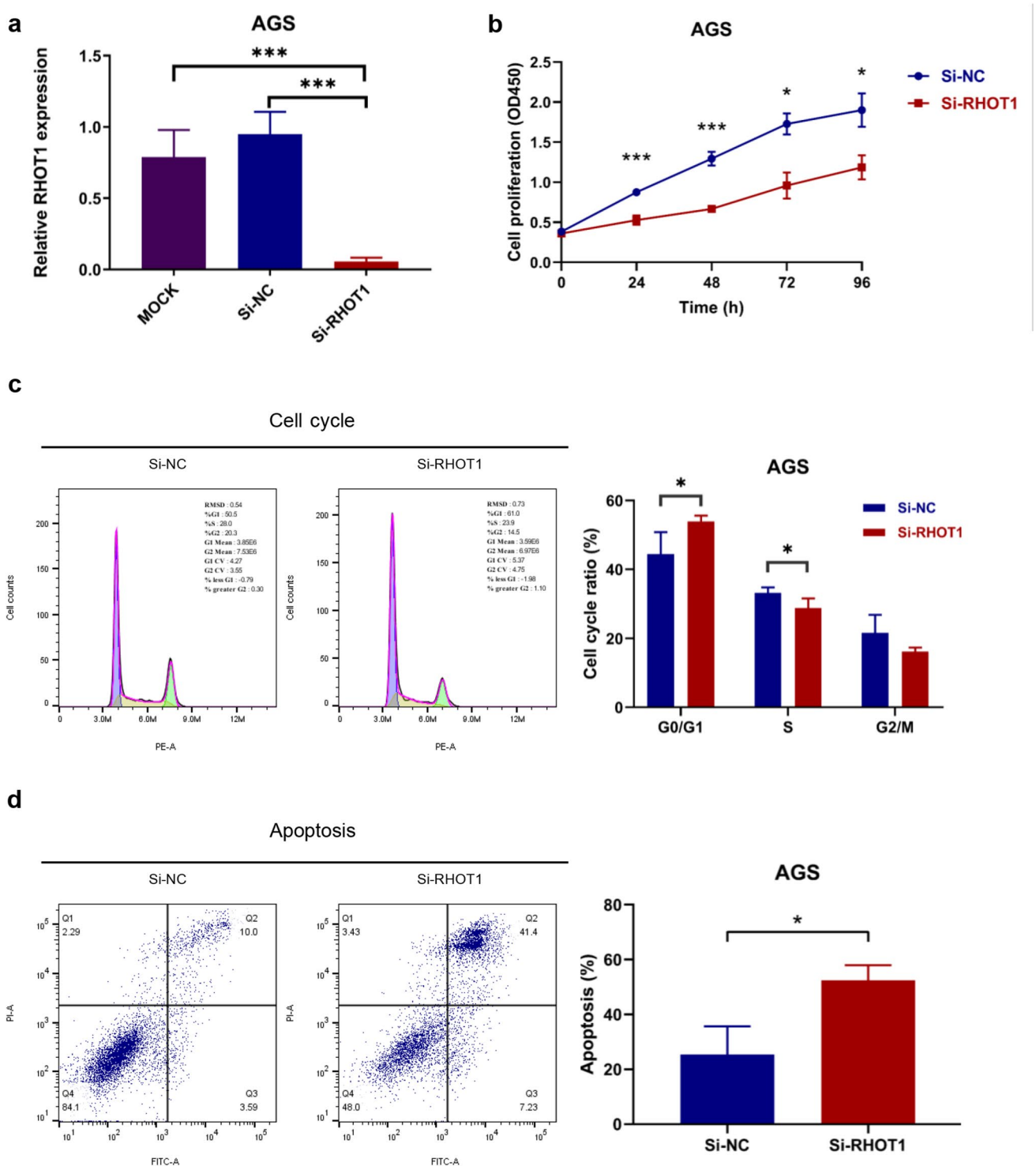

Fig. 4 Silencing RHOT1 diminished the capacities of the proliferation of GC cells arrested the cell cycle and promoted apoptosis. **a** Utilizing qRT-PCR assay, si-RHOT1 was effectively silenced in AGS cells. **b** It was observed from the CCK-8 assay, silencing RHOT1 declined the proliferation of AGS cells. **c** The use of cytometry analysis indicated that silencing RHOT1 arrested cell cycle progression and **d** promoted apoptosis in AGS cells. $^{*}P<0.05$, $^{**}P<0.01$, $^{***}P<0.001$, $n=3$

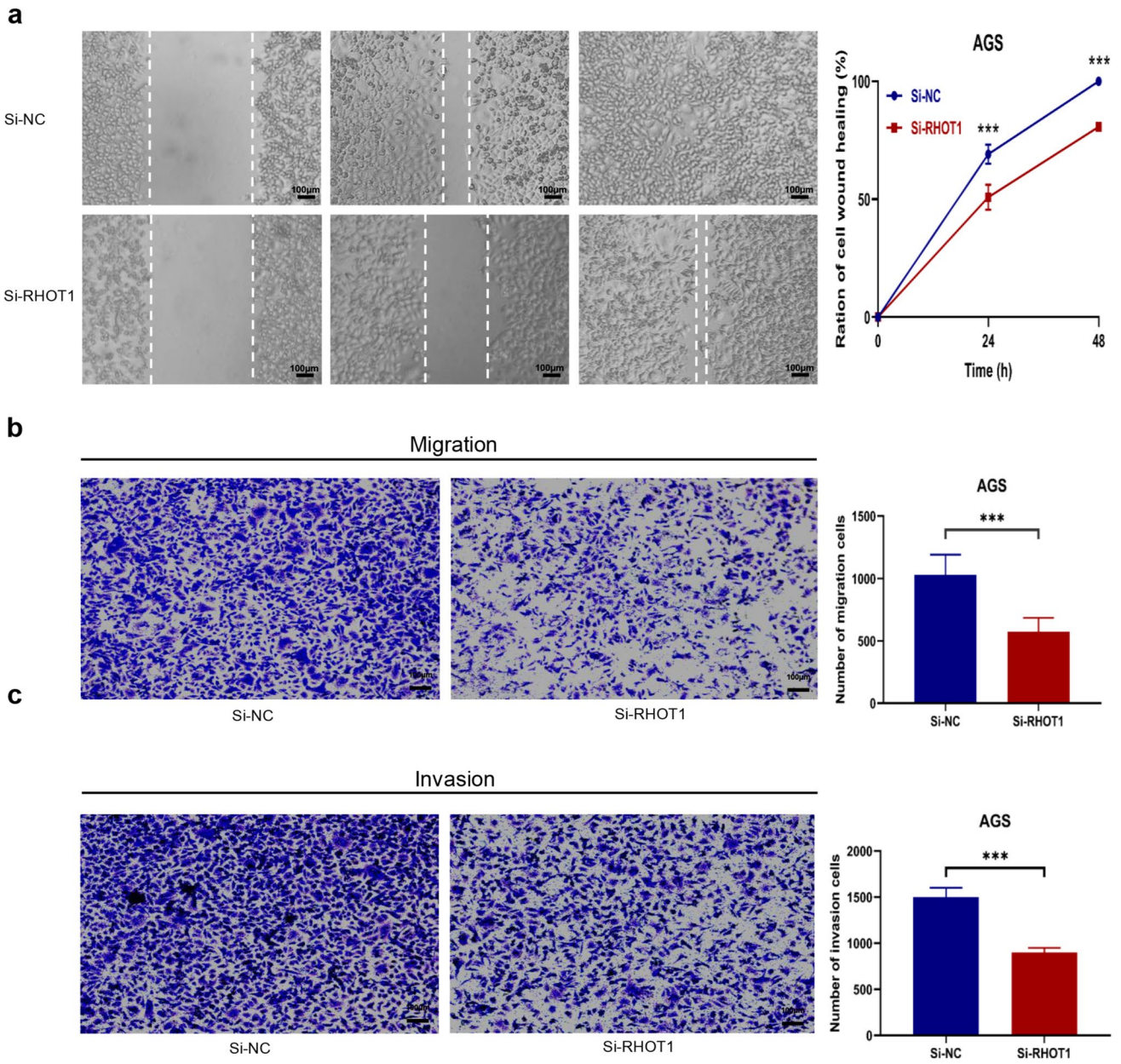

Fig. 5 Silencing RHOT1 inhibited the migration and invasion of GC cells. **a** The scratch wound assay observed that silencing RHOT1 expression inhibited the migratory capacity of AGS cells. **b** The transwell migration assay observed that silencing RHOT1 expression inhibited the potential migration capacity of AGS cells. **c** The transwell invasion assay observed that silencing RHOT1 expression decreased the potential invasion capacity of AGS cells. $*P<0.05$, $**P<0.01$, $***P<0.001$, $n=3$

a wound-healing assay to assess cell migration capacity after silencing RHOT1 in AGS cells. The results demonstrated a significant reduction in wound healing capacity in the si-RHOT1 group compared to the NC group (Fig. 5a). Concurrently, we executed the transwell migration assay. The graph indicated a significant decrease in the migration capacity of the si-RHOT1 group compared to the NC group (Fig. 5b). Our results demonstrated that the si-RHOT1 group had a considerably reduced invasion ability compared to the NC group (Fig. 5c). These findings suggested that the inhibition of RHOT1 resulted in reduced migration of AGS cells. Additionally, we assessed the invasion capacity of RHOT1 using a transwell invasion assay. It was demonstrated that RHOT1 could suppress the invasion capacity of AGS cells. The aforementioned results strongly suggested that the expression of RHOT1 could impact the migration and invasion of GC cells.

Discussion

As mentioned in the introduction, as a complex and heterogeneous tumor with multiple risk factors, GC was epidemiologically and histopathologically diverse worldwide and prone to migration and recurrence. Therefore, it is necessary to identify biomarkers for early diagnosis and explore the molecular mechanisms of gastric cancer progression [19]. Currently, limited research is exploring the role of RHOT1 in various tumors. In our previous investigation [13], we studied the expression of RHOT1 in GC tissues. In this study, we utilized bioinformatics and verified cytology assays to investigate the role of RHOT1 in GC. Firstly, we observed the expression of RHOT1 on the Pan-cancer level using TCGA data. Then, we analyzed the expression of RHOT1 in different groups, including normal tissues from GTEx data, to further understand its role. The study results indicated that RHOT1 was up-regulated in multiple types of tumors, including in GC tissues compared to the Normal group. These findings are consistent with our observation of RHOT1 up-expression in AGS, MGC-803, and SNU-1 cell lines compared to the GES-1 cell line through qPCR analysis. Furthermore, we observed varied expression levels of RHOT1 among different pathological factor groups in TCGA clinical samples data. After analyzing the survival rates of GC patients, we discovered that individuals with up-expression displayed shorter survival rates. We observed a correlation between RHOT1 expression and various pathological factors, in addition to survival rates. Therefore, RHOT1 has the potential to become a diagnostic and prognostic biomarker for GC. The result was consistent with what Jiang found in pancreatic cancer research [10]. We conjectured that RHOT1 acted as an oncogene that impacted GC progression, which was consistent with Li's research on the role of RHOT1 in pancreatic cancer [11]. Recently, many molecules have been reported to play a role in GC progression, including proliferation, invasion, and migration. For instance, CS synthase 3 (CHSY3) function in GC was associated with immune infiltration and promoted proliferation and migration in GC [20]; Vacuolar protein sorting-associated protein 35 (VPS35) enhanced epidermal growth factor receptor (EGFR) inhibitor response and promoted cell proliferation via EGFR recycling in GC [21]; Flotillin-1 (FLOT1) regulated breast cancer antiestrogen resistance 1 (BCAR1) phosphorylation and translocation. They were closely related to the poor outcome of GC patients. BCAR1-mediated FLOT1-induced GC progression and metastasis through ERK signaling [22]. We performed in vitro experiments to investigate the function of RHOT1 in GC. Silencing of RHOT1 mRNA significantly decreased the proliferation capacity of AGS cells, arrested them in the G0/G1 phase, and led to a decrease in migration and invasion capacity while increasing apoptosis. These results suggest that RHOT1 may be involved in multiple malignant biological behaviors of GC cells. Researchers thought that the RHOT1 protein could refine actin and tubulin-controlled mitochondrial movement and placement governing cell proliferation [23], it was consistent with our results.

Next, we sought to investigate the mechanism by which RHOT1 affected the biological behavior of GC cells. RHOT1, a key member of the atypical Rho GTPase family, played a critical role in maintaining mitochondrial and apoptotic homeostasis [6]. Previous reports demonstrated that RHOT1/2 can be ubiquitinated by Parkin at the outer mitochondrial membrane, thus impacting mitochondrial movement [24]. The movement of mitochondria came to a halt, which facilitated the progression of mitophagy for the elimination of impaired mitochondria [9]. Additionally, certain studies discovered a direct interaction between RHOT1 protein and PINK1 protein directly [25–27]. Researcher Birsa also observed that the protein of RHOT1 was ubiquitinated more early depending on PINK1 and Parkin proteins after mitochondria were destroyed, compared with RHOT2 [27]. Researchers Hsieh et al. demonstrated that RHOT1 was the one of earliest proteins that damaged mitochondria and obliterated them [28]. In addition, Agarwal proposed that the Myc gene was a ubiquitous oncogene that accelerates the development of aggressive cancer [12]. It operated through a network of genes responsible for the subcellular trafficking of mitochondria, which contained the atypical mitochondrial GTPases RHOT1 and RHOT2. Deregulation of this pathway disrupted mitochondrial dynamics obstructed subcellular organelle movements, and inhibited the recruitment of mitochondria to the cortical cytoskeleton of tumor cells. Consequently, Myc's regulation of mitochondrial trafficking could promote the motility and metastasis of tumor cells. These findings demonstrated that degraded RHOT1 protein may hinder mitochondrial motion after destruction, which may occur in GC. Furthermore, numerous pieces of evidence indicated that RHOT1 played a crucial role in the PINK1/Parkin pathway and validated some ubiquitinated sites [24]. Furthermore, the ubiquitination of RHOT1 protein might have additional functions [27]. Additionally, we inferred that RHOT1 was closely linked with PINK1 and Parkin, where PINK1 and Parkin were core proteins in the mitophagy pathway [29]. Based on the location of RHOT1 on the mitochondrial membrane and the ubiquitination of the RHOT1 protein, there may be a link to Parkin translocation and mitophagy. Therefore, we postulate that RHOT1 could impact the biological behaviors of GC through the mitophagy pathway.

This study initially used bioinformatics to demonstrate that an up-regulation of RHOT1 expression may influence

the prognosis of patients with GC. Subsequently, experiments were performed to verify that RHOT1 functions as an oncogene with the capacity to promote proliferation, migration, and invasion in GC cell lines. Moreover, the possibility is that RHOT1 may influence the biological behavior of GC cells through the mitophagy pathway. A future goal is to explore the mechanisms behind these phenomena.

Conclusion

RHOT1 expression was found to be up-regulated in GC and was positively correlated with patient prognosis. The expression of RHOT1 also appeared to affect the biological functions of GC cells, specifically apoptosis, proliferation, invasion, and migration. RHOT1 has the potential to become a valuable biomarker for early diagnosis and prognosis assessment of GC. Additionally, it may also serve as a novel therapeutic target for GC treatment.

Supplementary Information The online version contains supplementary material available at https://doi.org/10.1007/s12033-024-01107-8.

Funding This study was supported by the Doctoral Start-up Foundation of Liaoning Province, China (2022-BS-340); and the Supporting Project for Undergraduate Research project of Shenyang Medical College, China (20229010).

Data availability The original data in the manuscript were downloaded from the official websites of TCGA (https://portal.gdc.cancer.gov/) and GTEx (https://gtexportal.org/home/). TCGA and GTEx RNA-seq data in TPM format were obtained from UCSC XENA (https://xenabrowser.net/datapages/). Thanks to Xiantao Academic (www.xiantao.love) for providing the R language analysis platform.

Declartions

Conflict of interest The authors have no competing interests to declare that are relevant to the content of this article.

Ethical Approval This is an observational study. The Shenyang Medical College Research Ethics Committee has confirmed that no ethical approval is required.

References

1. Sung, H., & Ferlay, J. (2021). Global Cancer Statistics 2020: GLOBOCAN Estimates of Incidence and Mortality Worldwide for 36 Cancers in 185 Countries. *CA: A Cancer Journal for Clinicians, 71*, 209–249.
2. Rezaei, Z., & Ranjbaran, J. (2022). Identification of early diagnostic biomarkers via WGCNA in gastric cancer. *Biomedicine & Pharmacotherapy, 145*, 112477.
3. Karimi, P., & Islami, F. (2014). Gastric cancer: Descriptive epidemiology, risk factors, screening, and prevention. *Cancer Epidemiology, Biomarkers & Prevention, 23*, 700–713.
4. Hoshi, H. (2020). Management of gastric adenocarcinoma for general surgeons. *Surgical Clinics of North America, 100*, 523–534.
5. Swan, R., & Miner, T. J. (2006). Current role of surgical therapy in gastric cancer. *World Journal of Gastroenterology, 12*, 372–379.
6. Fransson, A., & Ruusala, A. (2003). Atypical Rho GTPases have roles in mitochondrial homeostasis and apoptosis. *Journal of Biological Chemistry, 278*, 6495–6502.
7. Fransson, S., & Ruusala, A. (2006). The atypical Rho GTPases Miro-1 and Miro-2 have essential roles in mitochondrial trafficking. *Biochemical and Biophysical Research Communications, 344*, 500–510.
8. Macaskill, A. F., & Brickley, K. (2009). GTPase dependent recruitment of Grif-1 by Miro1 regulates mitochondrial trafficking in hippocampal neurons. *Molecular and Cellular Neuroscience, 40*, 301–312.
9. Wang, X., & Winter, D. (2011). PINK1 and Parkin target Miro for phosphorylation and degradation to arrest mitochondrial motility. *Cell, 147*, 893–906.
10. Jiang, H., & He, C. (2012). RhoT1 and Smad4 are correlated with lymph node metastasis and overall survival in pancreatic cancer. *PLoS ONE, 7*, e42234.
11. Li, Q., & Yao, L. (2015). Role of RHOT1 on migration and proliferation of pancreatic cancer. *American Journal of Cancer Research, 5*, 1460–1470.
12. Agarwal, E., & Altman, B. J. (2019). Myc regulation of a mitochondrial trafficking network mediates tumor cell invasion and metastasis. *Molecular and Cellular Biology, 39*, e00109-119.
13. Peng, Y. Y., & Sun, D. (2022). Hsa_circ_0005230 is up-regulated and promotes gastric cancer cell invasion and migration via regulating the miR-1299/RHOT1 axis. *Bioengineered, 13*, 5046–5063.
14. Guo, Q., & Zhao, L. (2023). Integrated pan-cancer analysis and experimental verification of the roles of tropomyosin 4 in gastric cancer. *Frontiers in Immunology, 14*, 1148056.
15. Shi, Y., & Wang, Y. (2023). Crosstalk of ferroptosis regulators and tumor immunity in pancreatic adenocarcinoma: Novel perspective to mRNA vaccines and personalized immunotherapy. *Apoptosis, 28*, 1423–1435.
16. Liu, J., & Lichtenberg, T. (2018). An integrated TCGA pan-cancer clinical data resource to drive high-quality survival outcome analytics. *Cell, 173*, 400–416.
17. Ji, X., & Lee, Y. J. (2022). Characterization of cell cycle and apoptosis in Chinese hamster ovary cell culture using flow cytometry for bioprocess monitoring. *Biotechnology Progress, 38*, e3211.
18. Fox, M. H. (1980). A model for the computer analysis of synchronous DNA distributions obtained by flow cytometry. *Cytometry, 1*, 71–77.
19. Conti, C. B., & Agnesi, S. (2023). Early Gastric cancer: update on prevention, diagnosis and treatment. *International Journal of Environmental Research and Public Health, 20*, 2149.
20. Huang, X., & Liu, Y. (2023). CHSY3 promotes proliferation and migration in gastric cancer and is associated with immune infiltration. *Journal of Translational Medicine, 21*, 474.
21. Yu, J., & Feng, H. (2023). VPS35 promotes cell proliferation via EGFR recycling and enhances EGFR inhibitors response in gastric cancer. *eBioMedicine, 89*, 104451.
22. Wang, R., & Huang, W. (2023). FLOT1 promotes gastric cancer progression and metastasis through BCAR1/ERK signaling. *International Journal of Biological Sciences, 19*, 5104–5119.
23. Lopez-Domenech, G., & Covill-Cooke, C. (2018). Miro proteins coordinate microtubule- and actin-dependent mitochondrial transport and distribution. *EMBO Journal, 37*, 321–336.
24. Safiulina, D., & Kuum, M. (2019). Miro proteins prime mitochondria for Parkin translocation and mitophagy. *EMBO Journal, 38*, e99384.
25. Weihofen, A., & Thomas, K. J. (2009). Pink1 forms a multiprotein complex with Miro and Milton, linking Pink1 function to mitochondrial trafficking. *Biochemistry, 48*, 2045–2052.

26. Grossmann, D., & Berenguer-Escuder, C. (2019). Mutations in RHOT1 disrupt endoplasmic reticulum-mitochondria contact sites interfering with calcium homeostasis and mitochondrial dynamics in Parkinson's disease. *Antioxidants & Redox Signaling, 31*, 1213–1234.
27. Birsa, N., & Norkett, R. (2014). Lysine 27 ubiquitination of the mitochondrial transport protein Miro is dependent on serine 65 of the Parkin ubiquitin ligase. *Journal of Biological Chemistry, 289*, 14569–14582.
28. Hsieh, C. H., & Li, L. (2019). Miro1 marks Parkinson's disease subset and miro1 reducer rescues neuron loss in Parkinson's models. *Cell Metabolism, 30*, 1131–1140.
29. Schwarz, L., & Fitzgerald, J. C. (2022). Steady-state levels of miro1 linked to phosphorylation at serine 156 and mitochondrial respiration in dopaminergic neurons. *Cells, 11*, 1269.